R-590-PR
October 1970
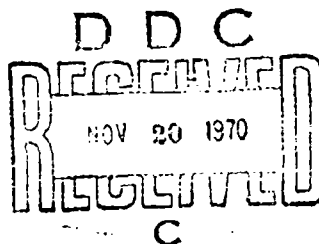
USE OF SCATTERING TECHNIQUES IN CLOUD MICROPHYSICS RESEARCH I. THE AUREOLE METHOD

D. Deirmendjian

A Report prepared for

UNITED STATES AIR FORCE PROJECT RAND

D D C

NOV 20 1970

C

Rand
SANTA MONICA, CA 90406

47

R-590-PR
October 1970

USE OF SCATTERING TECHNIQUES IN CLOUD MICROPHYSICS RESEARCH I. THE AUREOLE METHOD

D. Deirmendjian

A Report prepared for

UNITED STATES AIR FORCE PROJECT RAND

Rand

PREFACE

Scattering techniques and processes are receiving increasing attention in problems of reconnaissance; visibility; infrared imaging; turbidity; cloud physics; radiation balance at the surface, troposphere, and stratosphere; climatic change and modification, and many others.

Rand is continually exploring useful applications of this sensitive technique to problems of interest to the Air Force, DoD, and national environmental agencies. The present report is intended to improve estimates of the nature and degree of atmospheric turbidity on the basis of solar aureole measurements.

This is the first in a series that will evaluate existing observations and studies in the light of analytical techniques developed at Rand. Related Rand publications include R-407-PR, *Tables of Mie Scattering, Cross Sections and Amplitudes;* R-422-PR, *Complete Microwave Scattering and Extinction Properties of Polydispersed Cloud and Rain Elements;* R-456-PR, *Electromagnetic Scattering on Spherical Polydispersions.*

SUMMARY

One of the best uses of the scattering technique is the detection of small quantities of aerosol particles in an otherwise clear atmosphere. Under such conditions of very low turbidity, this is accomplished by careful observations of the aureole around the sun, that is, the circular region centered around the sun in which the sky brightness is higher than elsewhere.

In this report we re-examine the aureole theory in the form of a first-order perturbation of the well-known Rayleigh scattering field. We show that, with the use of the polydisperse scattering models proposed in a previous report,[*] the major features of the observed aureole may be faithfully reproduced without difficulty. By means of examples, we illustrate the differences between the aureole observed when the sun is high above the horizon and when it is close to the horizon. Similarly, we examine the differences produced by considering nonabsorbing and highly absorbing aerosols. In the latter case it is shown that considerable amounts of incident and diffuse radiation may be lost by absorption within the aerosols themselves.

Our principal conclusions are: (a) that the degree of atmospheric turbidity can best be assessed by comparing the deviations of sky brightness within a ring of radius $40°$ around the sun with the brightness corresponding to an equivalent Rayleigh atmosphere, and (b) that the nature of the size distribution of an atmospheric aerosol is closely related to the brightness gradient within a disc of radius $10°$ around the sun. Both these effects may be analyzed in terms of turbidity models based on polydispersions of Mie particles.

The present method, which is appealing in its simplicity and physical clarity, should be useful in providing rough estimates of the effects of various amounts and types of turbidity on the radiation budget of the earth-atmosphere system, and hence ultimately of the climatic effects, if any, of secular changes in turbidity.

---

[*]See Deirmendjian (1969) in the list of references.

ACKNOWLEDGMENTS

CONTENTS

1. INTRODUCTION

One of the important problems of atmospheric diagnostics is the detection of very small amounts of aerosols and other particulates and of small changes in their concentration, size, and composition. Continuing previous work by the author in this area, contained in several Rand Memoranda and Reports, we will here re-examine the ability of the aureole method to do this, using specific examples based on previously described and well-tested models of turbidity (Deirmendjian, 1969).[*]

In this and subsequent studies we will try to assess the degree of validity of the models in the face of available new experimental data obtained in the laboratory and in the atmosphere.

In general, we use the term "cloud microphysics" in the broader sense, to include natural and artificial condensation nuclei, the formation and dissipation of clouds, tropospheric and stratospheric aerosol layers not necessarily related to cloud formation, as well as the precipitation process *per se*. In all these areas, scattering techniques have proved very useful, especially when multiple scattering and radiative transfer effects are negligible. The unique determination of the properties of an aggregate of particles is difficult enough, even under conditions of pure primary scattering, and our discussion will be confined to this latter case.

----

[*] Hereafter referred to as ESSP.

2. THE AUREOLE OR SMALL-ANGLE SCATTERING METHOD

2.1 Background

The aureole around the sun and moon has been known to be a reliable indicator of the presence of aerosol layers in the atmosphere. The reason, of course, is that the diffraction-like forward scattering of light waves by three-dimensional particles, of a finite size relative to the wavelength, is so efficient that a relatively small number of particles suffices to produce the region of enhanced brightness over the general skylight background, known as the aureole. This same mechanism is responsible for the brighter portions of the zodiacal light at small angular distances from the sun, indicating the presence of micron-size "dust" particles in circumsolar space.

At the time of this author's initial interest in the subject (Deirmendjian 1956, 1957, 1959), the available observational and experimental material was rather limited. Since that time some additional work has been published, both on the natural phenomenon around the sun and on that produced by means of artificial sources allowing more systematic measurements. In examining these data a question of considerable practical importance is the ability to deduce *some* reliable information on the particle composition, shape, size, and size range from the aureole brightness and gradient alone. This, despite the fact that, on purely theoretical grounds, it would seem that unique solutions to this *inverse problem* may not exist. Nevertheless, continued efforts in this direction are well worthwhile because measurements are relatively easy to perform with the sun as a source, as well as with some of the new sources and detectors now available. A set of carefully and systematically obtained data on laboratory controlled samples will help settle certain questions which cannot be resolved by a theoretical treatment alone, such as:

(a) With what degree of confidence may one use the results of the scattering theory for spherical particles (Mie theory) as an approximation to the scattering by irregular particles in the aureole region? This could be accomplished by making

observations of the aureole produced by fine powders com-
posed of particles of known shape, index of refraction, and
size distribution, and comparing the observations with the
results of Mie theory for equivalent spherical particles.

(b) Under what conditions does multiple scattering modify and
eventually suppress the aureole in diffuse transmission
through highly forward-scattering media? Here it would be
necessary to measure the aureole through spherical water-
droplet clouds, keeping the size distribution constant in
each case and varying the depth or droplet concentration.
When performed at various wavelengths, including the infra-
red region, such measurements would provide the necessary
information as a function of optical thickness and albedo
of single scattering.

(c) How does the size-distribution function determine the char-
acteristics of the aureole for various kinds of spherical
particles? This question also could be answered by measure-
ments of a known medium, such as water droplets, if one
could control the actual size distribution. The results
would help check the validity of some of the proposed model
size-distributions for various cloud types, as well as de-
termine the best spectral region for aureole measurements
to detect particular aspects of condensation, cloud forma-
tion, and precipitation.

(d) To what extent do polarization measurements in the aureole
region reduce the uncertainties in the determination of the
physical properties of the scatterers?

Reliable answers to these and similar questions will greatly en-
hance the value of scattering techniques as diagnostic tools in cloud
microphysics research.

2.2 The Skylight Aureole around the Sun

2.21 The aureole as a perturbation of the Rayleigh field: non-absorbing aerosols.
To discuss observational data within an appropriate

theoretical framework, it will be useful to recall some pertinent concepts and parameters, and to describe those of their properties that are relevant to observed quantities. For simplicity and economy we shall follow the notations and definitions used in our own previous work. In particular, let us start by considering the differential equation which describes the singly scattered field in an *optically thin medium* illuminated by a constant parallel flux of electromagnetic energy from a given direction (ESSP, p. 96), that is,

$$\frac{d\underset{\sim}{I}(\tau,\theta,\zeta_o)}{\sec\,\zeta\,d\tau} = \underset{\sim}{I}(\tau,\theta,\zeta_o) - \frac{\varpi(\tau)}{4\pi}\,\underset{\sim}{P}(\tau,\theta)\cdot\underset{\sim}{F}_o\exp(-\,\tau\,\sec\,\zeta_o) \tag{1}$$

written in vector form, where $\underset{\sim}{F}_o$ is the Stokes vector of the incident radiation, $\underset{\sim}{I}$ is the Stokes vector of the local diffuse radiation, and and $\dfrac{\underset{\sim}{P}}{4\pi}$ is the four-by-four normalized Stokes scattering matrix for a sample of the scattering medium. This equation is already specialized to the case of a plane-stratified medium in which the direction of the incident radiation is given by a zenith distance ζ_o, that of the emergent by ζ (both measured from the normal to the plane of stratification), and a scattering angle θ determined by these two directions. Further, Eq. (1) is confined to the principal plane through the normal and incident directions, the radiation field being symmetrical with respect to this plane. The solutions to this first-order linear differential equation are well known, and may be written in the form *(loc. cit.)*:

$$\underset{\sim}{I}_{tr}(\tau_1;\zeta_o,\zeta) = \frac{\varpi}{4\pi}\,\underset{\sim}{P}(\theta)\,\cdot$$

$$\underset{\sim}{F}_o\,\frac{\sec\,\zeta}{\sec\,\zeta - \sec\,\zeta_o}\left[\exp(-\tau_1\,\sec\,\zeta_o) - \exp(-\tau_1\,\sec\,\zeta)\right] \tag{2}$$

$$\underset{\sim}{I}_{re}(\tau_1;\zeta_o,\zeta) = \frac{\varpi}{4\pi}\,\underset{\sim}{P}(\theta)\,\cdot$$

$$\underset{\sim}{F}_o\,\frac{\sec\,\zeta}{\sec\,\zeta - \sec\,\zeta_o}\left\{1 - \exp\left[-\tau_1(\sec\,\zeta_o + \sec\,\zeta)\right]\right\} \tag{3}$$

for the transmitted and reflected diffuse quasi-monochromatic radiation, respectively, in a medium strictly homogeneous with respect to its scattering properties as specified by the albedo of single scattering ϖ, and by $\underline{P}(\theta)$. The normal optical thickness τ_1, in Eqs. (2) and (3), in the case of the earth's atmosphere and an observer on or very close to the surface, may be expressed by the integral

$$\tau_1(h_1) = -\int_{h_1}^{\infty} \beta_{ex}(h) \, dh \tag{4}$$

where $\beta_{ex}(h)$ is the volume extinction coefficient and h is vertical height measured from the location of the observer in the case of transmission, or from the actual earth's surface below the observer, in the case of reflected light.

The solutions (2) and (3) can be used to describe the sunlit skylight or earthlight as seen by an observer not far from the surface, *only* as an initial approximation to the brightness of a very clear atmosphere, provided we confine ourselves to wavelengths $\lambda \geq 0.7$ μm (or optical thickness $\tau_1 \leq 0.10$) and assume that surface reflection effects are negligible. Even so, there are very few places in the above-mentioned spectral region where scattering is the dominant mechanism and where absorption is a slowly varying function of wavelength. In general, in regions where gaseous absorption bands can be neglected, it is clear that the atmosphere is not homogeneous with respect to scattering properties. Each element of the scattering matrix must then be written in the weighted form (ESSP, p. 99)

$$P_j(\theta,h) = \frac{\beta_{scR}(h) \, P_{jR}(\theta) + \beta_{scM}(h) \, P_{jM}(\theta)}{\beta_{sc}(h)} \tag{5}$$

with the subscripts R and M denoting Rayleigh (molecular) and Mie (aerosol) components respectively, and "sc" the scattering part of the extinction coefficient, so that

$$\beta_{sc}(h) = \beta_{scR}(h) + \beta_{scM}(h) \tag{6}$$

and

$$\beta_{sc}(h) + \beta_{ab}(h) = \beta_{ex}(h) \tag{7}$$

Similarly, the albedo of single scattering will in general be a function of h, and hence of τ, or

$$\varpi(h) = \frac{\beta_{scR}(h) + \beta_{scM}(h)}{\beta_{ex}(h)} \tag{8}$$

and there may be no analytical integrals for Eq. (1), such as Eqs. (2) and (3), unless the above parameters are special functions of h.

However, *if* second- and higher-order scattering effects can be neglected, one may solve for two individual equations, such as (1), written separately for a Rayleigh and aerosol atmosphere, respectively, and add the solutions for each element of the Stokes vector, to obtain a resultant vector for the mixed atmosphere. The use of first-order scattering only, in the Rayleigh component, would be rather unreasonable, since there exist good numerical tables (Coulson et al., 1960; Sekera and Kahle, 1966) based on well-tested theory, which take into account all relevant orders of scattering for the case $\varpi(h) = 1$.

One way to make use of these results in evaluating the first-order effects of moderate atmospheric turbidity is to treat such effects as a perturbation of the Rayleigh scattering mechanism (Sekera, 1956). The method has been used (Deirmendjian, 1956) in an attempt to reproduce the sun's aureole in a first approximation. The agreement of the initial attempt with observation was only fair, owing to an inaccurate evaluation of the forward-scattering part of the aerosol component, rather than to deficiencies in the method. In order to better evaluate its merits, we will present below some sample calculations of the aureole corresponding to a moderately turbid sky based on the available more accurate values of the scattering matrix elements $P_{jM}(\theta)$.

Briefly the method consists in defining a perturbation scattering matrix $\underset{\sim}{P}_{jD}(\theta)$ whose elements are given by the differences

$$P_{jD}(\theta) = P_{jM}(\theta) - P_{jR}(\theta) \qquad (9)$$

and which obey the condition that the contribution to the net flux integrated over all directions around a point must vanish; that is,

$$\frac{1}{8\pi} \int_{\Omega} \left[P_{1D}(\theta) + P_{2D}(\theta) \right] d\omega = 0 \qquad (10)$$

This follows from the fact that the corresponding integrals of the elements of the matrices on the right-hand side of Eq. (9) by definition are normalized to unity. From this, in turn, it follows that the integrand in Eq. (10) must be negative in certain directions, a property which is contrary to the concept of "intensity," a positive quantity also by definition. Hence the matrix $\underset{\sim}{P}_D(\theta)$ must be considered to represent a *virtual* scattering process, corresponding to no real particles, and introduced only for mathematical convenience.

The elements of the scattering matrix for a sample of turbid air, given by Eq. (5), may then be written in the alternative form

$$P_j(\theta,h) = P_{jR}(\theta) + \frac{\beta_{scM}(h)}{\beta_{scR}(h) + \beta_{scM}(h)} P_{jD}(\theta) \qquad (11)$$

which is automatically in normalized form by virtue of Eq. (10), and where there is only a single weighting function or *turbidity coefficient* $f(\tau)$ such that

$$0 \le f(\tau) \equiv \frac{\beta_{scM}(h)}{\beta_{scR}(h) + \beta_{scM}(h)} < 1 \qquad (12)$$

This coefficient tends to vanish when the amount of aerosol particles is infinitesimal as far as the scattering properties of "pure" air are concerned. Such conditions are rarely approached in the troposphere near sea level and in the vicinity of urban areas.

When the matrix formed by Eq. (11) is introduced into the equation of radiative transfer for a scattering atmosphere with higher-order effects taken into account, it may be expressed as the sum of two equations, written respectively for the Rayleigh component $\mathbf{I}_R$ and a perturbation component $\mathbf{I}_D$. Each of these in principle may then be solved separately and the total field may be obtained by the addition of the two solutions in each case. *If* one considers only wavelengths where there is *no absorption either by molecules or aerosols,* one may use for the Rayleigh cmponent, for example, the well-known solutions of the conservative problem and their tabulations mentioned above. It should be borne in mind, however, that in the turbid case there is no unique, one-to-one correspondence between wavelength and the normal optical thickness. The latter in general will be a variable function of the type, total amount, and stratification of the turbidity, and hence it must be determined individually for each wavelength before interpolating in the Rayleigh tables for the corresponding optical thickness.

The complete equation for the perturbation component $\mathbf{I}_D$, written for the standard case (no reflecting boundaries) and limited to the principal vertical plane, takes the form (Deirmendjian, 1956, 1957),

$$\frac{d\mathbf{I}_D(\tau,\zeta,\zeta_o)}{\sec \zeta \, d\tau} = \mathbf{I}_D - \frac{f(\tau)}{4\pi} e^{-\tau \sec \zeta_o} \, \mathbf{P}_D (\theta) \cdot \mathbf{F}_o$$

$$- \frac{f(\tau)}{4\pi} \int_\Omega \mathbf{P}_D(\psi) \cdot \left[\mathbf{I}_R(\tau,\zeta',\phi') + \mathbf{I}_D(\tau,\zeta',\phi') \right] d\omega$$

$$- \frac{1}{4\pi} \int_\Omega \mathbf{P}_R(\psi) \cdot \mathbf{I}_D(\tau,\zeta',\phi') \, d\omega \qquad (13)$$

where ψ is the scattering angle between the direction ζ', ϕ' of the local diffuse field and the direction of the sought field, given by

the zenith angle ζ and the azimuth $\phi = 0$ or π, and the remaining symbols are as previously defined.

Equation (13), which is *valid only for nonabsorbing particles,* is in a form that allows a physical interpretation for each term and, in principle, is amenable to solutions in various approximations, depending on the particular aspect of the problem in which one is interested. For example if one disregards the terms on the right side of Eq. (13) containing integrals, one is neglecting higher-order effects due to the turbidity. The remaining differential equation

$$\frac{dI_D^{(1)}}{\sec \zeta \, d\tau} = I_D^{(1)} - \frac{f(\tau)}{4\pi} e^{-\tau \sec \zeta_o} P_D(\theta) \cdot E_o \tag{14}$$

when solved, will yield a first-order approximation $I_D^{(1)}$ to the perturbation field,[*] which accounts only for the primary scattering of sunlight according to the virtual mechanism represented by the matrix $P_D(\theta)$. In a cloudless atmosphere, with low to moderate turbidity, this approximation should be most suitable in estimating the total brightness field and sky color in the vicinity of the sun caused by the forward-scattering aerosols at angular distances up to 40° from the sun (cf. e.g. ESSP, p. 101). Since this region of the sky usually includes the two neutral points of skylight polarization, known as the Babinet's and Brewster's points, respectively, the first-order approximation obtained from Eq. (14), when added to the Rayleigh component, should provide a partial explanation of the fact that, in general, the observed positions of these points differ considerably from those given by the Rayleigh multiple-scattering theory (see e.g. Sekera, 1956; Deirmendjian, 1959).

_____

[*] Here we consider with Rozenberg (1968) that a zeroth approximation $I^{(o)}(\tau, \zeta_o)$ is equivalent to disregarding skylight entirely and considering only the insolation of the ground due to solar flux attenuated by the actual turbid atmosphere. The usefulness of this approximation in estimating, for example, the climatic effects of volcanic dust, etc., is obviously very doubtful.

If one is interested in the effects of turbidity on the skylight brightness and polarization field at large angular distances from the sun, the shape of the curves for the first two elements of the scattering matrix (5) or (11) for typically turbid air (ESSP, p. 101) indicates that the last two terms on the right-hand side of Eq. (13) cannot be neglected. In particular, the regions of maximum skylight polarization could be affected by the last term, which represents an additional Rayleigh type field arising from illumination of the air sample by the aureole region. If for the latter we substitute the first-order approximation mentioned above, we obtain a second-order approximation, $I_D^{(2)}$, to the perturbation field by solving the integro-differential equation

$$\frac{dI_D^{(2)}(\tau,\zeta,\zeta_o)}{\sec \zeta \, d\tau} = I_D^{(2)} - \frac{1}{4\pi} \int_\Omega P_R(\psi) \cdot I_D^{(1)}(\tau,\zeta_o,\zeta',\phi') \, d\omega \qquad (15)$$

where now the field $I_D^{(1)}$ for each position of the sun at each level throughout the atmosphere must be known for *all directions around the air sample,* and Eq. (14) must first be solved for all azimuths around the vertical both for diffusely transmitted *and* reflected sunlight. In the latter case the effects of ground reflection are not negligible and the integration of Eq. (14) becomes more cumbersome. An added difficulty in the solution of Eq. (15) is that the two factors in the integrand on the right side must be expressed in a single coordinate system.

At any rate, once the perturbation field I_D is obtained by some method, the total field should be given by

$$I(\lambda,\tau_1,\zeta_o,\zeta,\phi) = I_R(\lambda,\tau_1,\zeta_o,\zeta,\phi) + I_D(\lambda,\tau_1,\zeta_o,\zeta,\phi) \qquad (16)$$

to the degree of approximation governed by the quality of the assumptions.

2.22 Considerntion of absorbing aerosols. If we consider spectral regions where there is no broad-band molecular absorption but where there may be scattering absorption by aerosol particles, so that $\beta_{exM} > \beta_{scM}$, then the albedo for single scattering [Eq. (8)] may be expressed in the form

$$\varpi(\tau) = \frac{\beta_{scR} + \beta_{scM}}{\beta_{scR} + \beta_{exM}} < 1 \tag{17}$$

Let us retain the definitions of the previous section, including that of the *scattering* turbidity coefficient $f(\tau)$ as defined in Eqs. (11) and (12), and try to evaluate the effects of absorbing aerosols as a perturbation of the Rayleigh field. If the equation of transfer is again separated as in Section 2.21, the equation for the Rayleigh component now takes the form

$$\frac{d\,I_R}{\sec\zeta\,d\tau} = I_R(\tau,\zeta_0,\zeta,\phi) - \frac{\varpi(\tau)}{4\pi}\,P_R(\theta)\cdot F_0 e^{-\tau\,\sec\zeta_0}$$

$$- \frac{\varpi(\tau)}{4\pi}\int_\Omega P_R(\psi)\cdot I_R(\tau,\zeta',\phi')\,d\omega \tag{18}$$

which shows that the albedo of single scattering, given by Eq. (17), must be taken into account even when the Rayleigh scattering by the molecules is a nonabsorbing, conservative process. In general, tabulations of the solution to Eq. (18) do not exist for nonconservative Rayleigh atmospheres of finite optical thickness and for arbitrary values of $\varpi(\tau)$ as a function of position of sun and direction of skylight, except in special cases.

The complete equation for the perturbation field I_D in this case becomes

$$\frac{d \, I_D(\tau,\varpi,\zeta_0,\zeta)}{\sec \zeta \, d\tau} = I_D - \frac{\varpi(\tau)f(\tau)}{4\pi} \, e^{-\tau \sec \zeta_0} \, \underline{P}_D(\theta) \cdot \underline{E}_0$$

$$- \frac{\varpi(\tau)f(\tau)}{4\pi} \int_\Omega \underline{P}_D(\psi) \cdot \left[I_R(\tau,\zeta',\phi') + I_D(\tau,\zeta',\phi') \right] d\omega$$

$$- \frac{\varpi(\tau)}{4\pi} \int_\Omega \underline{P}_R(\psi) \cdot I_D(\tau,\zeta',\phi') \, d\omega \tag{19}$$

which is quite similar to Eq. (13) except for the albedo factor attached to all the process terms on the right-hand side. Here the turbidity coefficient $f(\tau)$ and perturbation matrix $\underline{P}_D$ are defined exactly as in the previous section, that is, by Eqs. (9) and (12).

A relation between $\varpi(\tau)$ and $f(\tau)$ may be found by considering (12) and (17), to wit

$$\varpi(\tau) \, f(\tau) = \frac{\beta_{scM}(\tau)}{\beta_{scR}(\tau) + \beta_{exM}(\tau)} \equiv \varpi_M(\tau) \tag{20}$$

where $\varpi_M(\tau)$, defined as above, may be considered a partial albedo of single scattering for the aerosol component. Similarly we may define another partial albedo $\varpi_R(\tau)$ by the relation

$$\varpi(\tau) \, [1 - f(\tau)] = \frac{\beta_{scR}}{\beta_{scR} + \beta_{exM}} \equiv \varpi_R(\tau) \tag{21}$$

so that we have

$$\varpi(\tau) = \varpi_R(\tau) + \varpi_M(\tau) \tag{22}$$

This separation may be useful in approximate treatments of the problem of absorbing aerosols.

On the basis of Eq. (19), we can make some preliminary statement about the aureole perturbation produced by absorbing aerosols: If the factor given by Eq. (20) is small, i.e., if $\varpi_M \ll \varpi_R$, then the

first-order approximation to the field, obtained by the solution of an equation similar to Eq. (14), will yield a rather weak primary aureole. When this is reintroduced into Eq. (19) to obtain higher-order effects, it is seen that the last term on the right may be more important than the preceding term, in its effects on both the overall brightness and on the polarization field.

At any rate, we shall not consider higher-order effects here, but will confine ourselves to some examples of the first-order field $\underset{\sim}{I}^{(1)}$ that are sufficient to describe the main features of the aureole.

2.23 Examples of first-order aureole for nonabsorbing aerosols.

Equation (14) is seen to be in the form of an inhomogeneous, ordinary differential equation of the first order, since the optical thickness τ is the only independent variable. Its standard solution, written for the Stokes vector of the perturbation field, is therefore given by an expression such as

$$\underset{\sim}{I}_{D}^{(1)}(\tau_1,\zeta_0,\zeta) = T_D(\tau_1,\zeta_0,\zeta)\, \frac{\underset{\sim}{P}_D(\theta) \cdot \underset{\sim}{F}_0}{4\pi} \tag{23}$$

where T_D is the positive number defined by the integral

$$T_D(\tau_1,\zeta_0,\zeta) \equiv \sec\zeta\; e^{-\tau_1 \sec\zeta} \int_0^{\tau_1} f(\tau)\, e^{-|\sec\zeta_0 - \sec\zeta|\tau}\, d\tau \tag{24}$$

The expression (24) may be considered as a transmission function for the perturbation, which takes into account both the attenuation and the enhancement produced by the amount of aerosols and atmosphere in the path of sunlight and scattered light. The integral in (24) cannot, in general, be evaluated in closed form. Usually both the size distribution and the nature of the aerosol particles vary with height -- and hence with optical thickness -- in a complicated manner, and the integration has to be performed numerically.

If both the size distribution $n(r)$ and the composition of the aerosol particles is independent of height and only their total number

N(h) per unit volume varies monotonically with height in some simple
manner, the problem of evaluating Eq. (24) may be considerably simpli-
fied. But even if the turbidity coefficient $f(\tau)$, as defined by Eq.
(12), should be an exponential function of the height h above the
ground, for example, it may still not be an explicit function of the
overall optical thickness τ, and again one has to use approximate
numerical and graphical methods to evaluate T_D. From actual observa-
tions, however (cf. Rozenberg, 1968), it appears that the aerosol con-
centration does not drop monotonically with height, but rather there is
a transition region between tropospheric and stratospheric aerosols
and a definite concentration maximum around 18 km.

In an initial attempt (Deirmendjian, 1956), numerical methods
were used on the basis of data then available on n(r) and N(h) in the
troposphere, to obtain reasonable estimates of T_D for some model dis-
tributions. However, the aureole brightness gradients and magnitudes
deduced for the skylight in the immediate neighborhood of the sun were
in error on two counts: (a) the so-called "main diffraction peak"
approximation, used in deriving the small-angle scattering part of
$\underset{\sim}{P}_M(\theta)$, *overestimated the brightness gradient*, especially since it was
used in conjunction with a power-law size distribution; and (b) the
magnitude of the perturbation field was *underestimated* for all direc-
tions by the factor $(4\pi)^{-1}$, that is, by at least one order of magni-
tude, as already pointed out elsewhere (Deirmendjian, 1964).

With the introduction of more meaningful size-distribution func-
tions for aerosols, first proposed by Deirmendjian (1963), and of ex-
act Mie calculations of $\underset{\sim}{P}_M$ based on such distributions (Deirmendjian,
1963, 1964, 1969), one should be able to obtain a better theoretical
approximation of the observed phenomenon of the clear-sky aureole,
particularly as to the absolute brightness, its gradient, and the
angular extent of the forward-scattering effects around the sun.

In order to correct the above-mentioned errors in the first-order
approximation to the aureole by means of the improved models, let us
consider a homogeneous atmosphere with *homogeneous turbidity*, as sug-
gested previously (cf. Deirmendjian, 1959, Appendix B). This is equi-
valent to replacing the actual vertical distribution of the aerosols

by a virtual distribution with a constant mixing ratio of particles
to molecules, so that the total numbers in a vertical column remain un-
changed. This amounts to setting

$$f(\tau) = f(\tau_1) = \frac{\tau_{1M}}{\tau_{1R} + \tau_{1M}} = \text{constant} \qquad (25)$$

where the normal optical thickness components τ_{1R} and τ_{1M} are given
by integrals of the type (4) using the appropriate values and vertical
distribution of the extinction coefficient for Rayleigh and aerosol
particles, respectively. The integral in Eq. (24) in this case can be
easily evaluated to get

$$T_D(\tau_1, \zeta_0, \zeta) = \frac{\sec \zeta}{|\sec \zeta - \sec \zeta_0|} f(\tau_1) \left| e^{-\tau_1 \sec \zeta_0} - e^{-\tau_1 \sec \zeta} \right| \qquad (26)$$

where the absolute-value symbols are inserted merely to indicate that
the whole expression is always positive. Introducing this into (23)
we have

$$I_D^{(1)}(\tau_1, \zeta_0, \zeta) = \frac{f(\tau_1)}{4\pi} P_D(\theta) \cdot E_0 \frac{\sec \zeta \left| e^{-\tau_1 \sec \zeta_0} - e^{-\tau_1 \sec \zeta} \right|}{|\sec \zeta - \sec \zeta_0|} \qquad (27)$$

which, except for the turbidity factor $f(\tau_1)$, is seen to be identical
to the solution (2) for primary scattering by the whole atmosphere
with $\varpi = 1$.

This simple solution (27) for the perturbation field should be
used only when the homogeneous turbidity model is a useful approxima-
tion, that is, (a) when we are interested only in the field at the
boundary of the atmosphere but not in its interior, and (b) for rela-
tively small values of ζ_0 and ζ, when neither the sun nor the points
in the sky considered are very close to the horizon, so that curvature
effects may be neglected in the atmospheric and aerosol stratification.

As an illustration of the method we consider the aureole produced
by what elsewhere we have called a haze-L type particle distribution,

given by (ESSP, p. 78)

$$n(r) = 4.976 \cdot 10^6 \, r^2 \, e^{-15.1186 \, \sqrt{r}} \qquad \qquad cm^{-3} \mu^{-1} \quad (28)$$

where r is the particle radius in microns and n(r) is the number of particles per cubic centimeter per one-micron increment in radius. Distribution (28) was normalized so that the integral over all radii yields exactly 100 particles per cm^3. For water particles with the above distribution, the scattering parameters have been evaluated for a number of wavelengths covering the visible and infrared continuum (ESSP, Tables T.16 to T.26). For the nonabsorbing case we must limit ourselves to the visible range where the model gives scattering (or extinction) coefficients of 0.0480 and 0.0395 per km at wavelengths of $\lambda 0.45$ and $\lambda 0.70$ micron, respectively.

To construct a model of the turbid atmosphere we consider 1.632 km of homogeneous aerosol, conforming to a haze-L model (that is, $1.632 \cdot 10^7$ particles per cm^2 column), mixed with the earth's standard atmosphere in order to closely approximate one of our initial models, called B (Deirmendjian, 1956, 1959), in the magnitude and wavelength dependence of the overall optical thickness and turbidity coefficient. In Fig. 1 we show the optical thickness of the Rayleigh, aerosol, and mixed atmosphere, respectively, as indicated by the labelled curves, in the range $0.32 \leq \lambda \leq 2.0\mu$. The Rayleigh part for nonabsorbing molecules, obeying the λ^{-4} law, is taken from Deirmendjian (1955), and the τ_M curve is adapted from the above-mentioned tables by fitting a smooth curve to the data points. The implied interpolation and extrapolation is justified on the basis of the smooth variation of the index of refraction in this region and the existence of weak liquid-water absorption bands which do not appreciably affect the extinction by scattering. The numerical values used for the sea-level total optical thickness, at two reference wavelengths, are shown below for convenience:
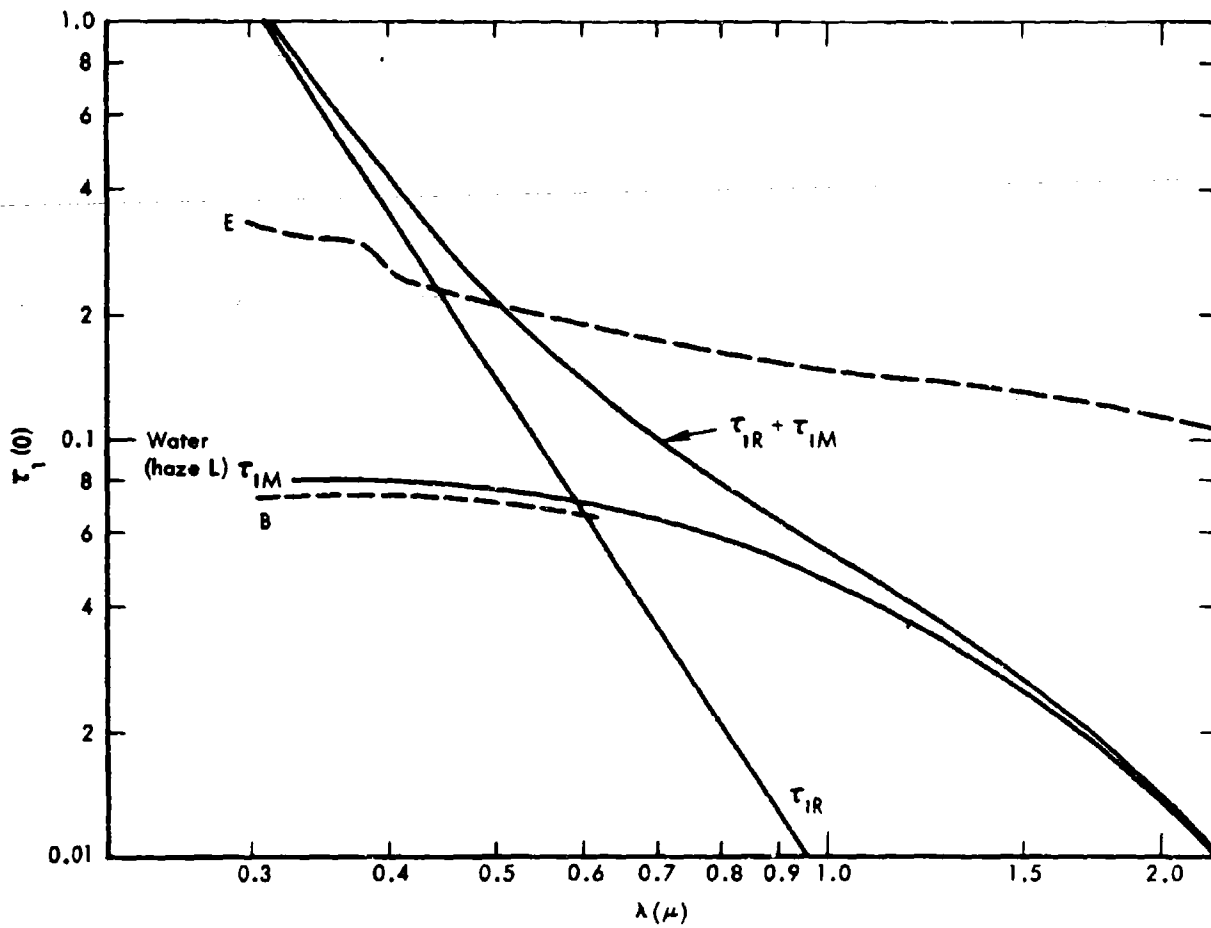
Fig. 1 -- Rayleigh and aerosol model components of normal optical
thickness at sea level.

	$\lambda 0.45\mu$	$\lambda 0.70\mu$
τ_{1R}	0.217	0.0355
τ_{1M} (Water "haze L")	0.0783	0.0645
τ_1	0.295	0.100
$f(\tau_1)$	0.265	0.645

The dashed line in Fig. 1, marked "B" is included to indicate the magnitude and shape of the old "model B" aerosol curve, mentioned above (limited to the visible range only) and to show its close similarity to the more complete haze-L model in the same region. Both these models represent a clear atmosphere with rather light turbidity, to be found near sea level and away from the influence of urban pollution sources. To get an idea of magnitudes, let us compare them with a so-called "clear standard atmosphere," proposed by Elterman (1964a,b), without necessarily implying that we agree with that author's choice of "standard" model. A model optical thickness curve, equivalent to our τ_{1M}, and corresponding to Elterman's (1964b) model, may be obtained by multiplying the latter's tabulated values of the sea-level aerosol attenuation coefficient by about 1.275 km. (This scale height is implied -- but not explicitly shown -- by the arithmetic of the other quantities tabulated by Elterman). The result is indicated by the dashed curve marked "E" in Fig. 1, and it is clear that in the vertical direction Elterman's model aerosol atmosphere is optically three times as thick as our example, regardless of the detailed stratification. (The Elterman values, corresponding to our τ_{1M} in this case, are 0.230 and 0.172 at $\lambda 0.45$ and 0.70μ, respectively. The differences are more pronounced in the infrared region. On the other hand, the number of aerosol particles in a vertical column of 1 cm^2 cross section through the atmosphere is $2.55 \cdot 10^7$ for Elterman's "standard" model, compared to $1.632 \cdot 10^7$ for our model. Their ratio is considerably smaller than that of the optical thicknesses, which indicates that Elterman's model assumes a greater proportion of large aerosol particles than ours.

Considering the optical thickness components represented by the
full lines in Fig. 1, we can distinguish three spectral regions in
the visible and near infrared, depending on the magnitude of $f(\tau)$ in
(25): a short-wavelength region in the blue and near ultraviolet,
for say $\lambda < 0.40\mu$, where the aerosol component is small and hence its
effect may be considered as a perturbation on the main Rayleigh radia-
tion field; a long-wavelength region with $\lambda > 0.9\mu$ in the infrared,
where the scattered field should he given mainly by the aerosol com-
ponent and a small Rayleigh perturbation which becomes negligible at
longer wavelengths; and an intermediate region $0.40 \le \lambda \le 0.9\mu$, where,
strictly speaking, both components are of equal or comparable impor-
tance and the problem should be treated accordingly. For our present
purposes, we shall evaluate the aureole by means of the perturbation
technique at two wavelengths in this intermediate region, with the un-
derstanding that the result for $\lambda 0.45\mu$ will be more valid than that
for $\lambda 0.70\mu$.

Since for the moment we are not interested in polarization ef-
fects, we need to know only the semi-sum of the first two elements of
the perturbation matrix $\underline{P}_D(\theta)$ to get the scattered intensity for un-
polarized incident sunlight. This is easily obtained from Eq. (9) by
finding the difference between the corresponding Mie and Rayleigh quan-
tities, or by setting

$$\tfrac{1}{2}(P_{1D} + P_{2D}) = \tfrac{1}{2}(P_{1M} + P_{2M}) - \tfrac{3}{4}(1 + \cos^2\theta) \tag{29}$$

where the first term on the right may be obtained for either wavelength
from the previously mentioned tables (ESSP, pp. 166-7) and the second
term is the corresponding Rayleigh quantity, independent of wavelength.
Sample values of Eq. (29) are shown in Table 1 for comparison with the
old estimates (Deirmendjian, 1959, Table 3, p. 231) and verification
of the discrepancies mentioned earlier.

All that remains in order to evaluate the scalar intensity $I_D = \tfrac{1}{2}(I_{1D} + I_{2D})$ of the perturbation field is to set $F_1 = F_2 = \tfrac{1}{2}$, for unit
unpolarized incident flux, find the values of $f(\tau_1)$ according to Eq. (25)

Table 1

NORMALIZED INTENSITY ELEMENT OF THE PERTURBATION MATRIX $\underset{\sim}{P}_D(\theta)$
FOR LIGHT TURBIDITY CONDITIONS

θ (degrees)	$\frac{1}{2}(P_{1D} + P_{2D})$		θ (degrees)	$\frac{1}{2}(P_{1D} + P_{2D})$	
	$\lambda 0.45\mu$	$\lambda 0.70\mu$		$\lambda 0.45\mu$	$\lambda 0.70\mu$
0	45.31	28.85	15	10.67	11.38
2.5	41.73	27.81	20	6.072	6.954
5	33.74	25.04	30	1.861	2.262
7.5	25.64	21.44	40	0.2939	0.4303
10	19.10	17.71	50	-0.3051	-0.2609

and the model, and compute the transmission function T_D from Eq. (26) for fixed values of ζ_o and a set of values of ζ corresponding to the range of scattering angles $\theta = |\zeta_o - \zeta|$ representative of the aureole perturbation, say $0° \leq \theta \leq 40°$. The result must then be added to the corresponding Rayleigh field $I_R = \frac{1}{2}(I_{1R} + I_{2R})$ to get an idea of the aureole sky around the sun.

The Rayleigh background may be estimated with good accuracy by interpolation using existing tables (Coulson et al., 1960, Table 1) for the normalized "intensity of downward radiation," after first dividing their tabulated values by π (the normalized incident flux assumed by these authors). For the present example we have chosen two positions of the sun, given by $\cos^{-1} 0.80$ and 0.20 or zenith distances of $36°52'$ and $78°28'$, respectively, to coincide with two of the standard values listed in the above-mentioned tables. To interpolate with respect to optical thickness (or wavelength) we used a so-called Lagrange (five-point) numerical interpolation scheme, pre-programmed into Rand's JOSS computer system. This was needed only for $\tau_1 = 0.295$ at $\lambda 0.45\mu$ (case for zero ground albedo), since the remaining value, $\tau_1 = 0.10$ at $\lambda 0.70\mu$, is a standard one used in the tabulations. The necessary interpolations with respect to optical thickness and to ζ cannot lead to any significant errors, since the Rayleigh skylight is known to be a slowly varying and smooth function of direction even in the vicinity of the sun (Deirmendjian and Sekera, 1953).

Both these components, the Rayleigh background and the first-order approximation, $I^{(1)} = I_R + I_D^{(1)}$, of its perturbed state in the aureole region, obtained as above, may be better appreciated by a graphical presentation than through numerical tables (see Appendix). In Figs. 2 and 3 the abscissas are plotted in values of $\sin \theta \equiv \sin |\zeta_o - \zeta|$, increasing linearly on either side of the position of the sun, given by ζ_o. The actual diameter of the sun, in these coordinates, is indicated by the parallel lines around the ordinate at ζ_o. For convenience we have labelled the lower horizontal frame in the zenith distance ζ, measured in degrees of arc, and the upper one in both $\sin \theta$ and θ. The ordinates are marked in the normalized intensities, plotted logarithmically.
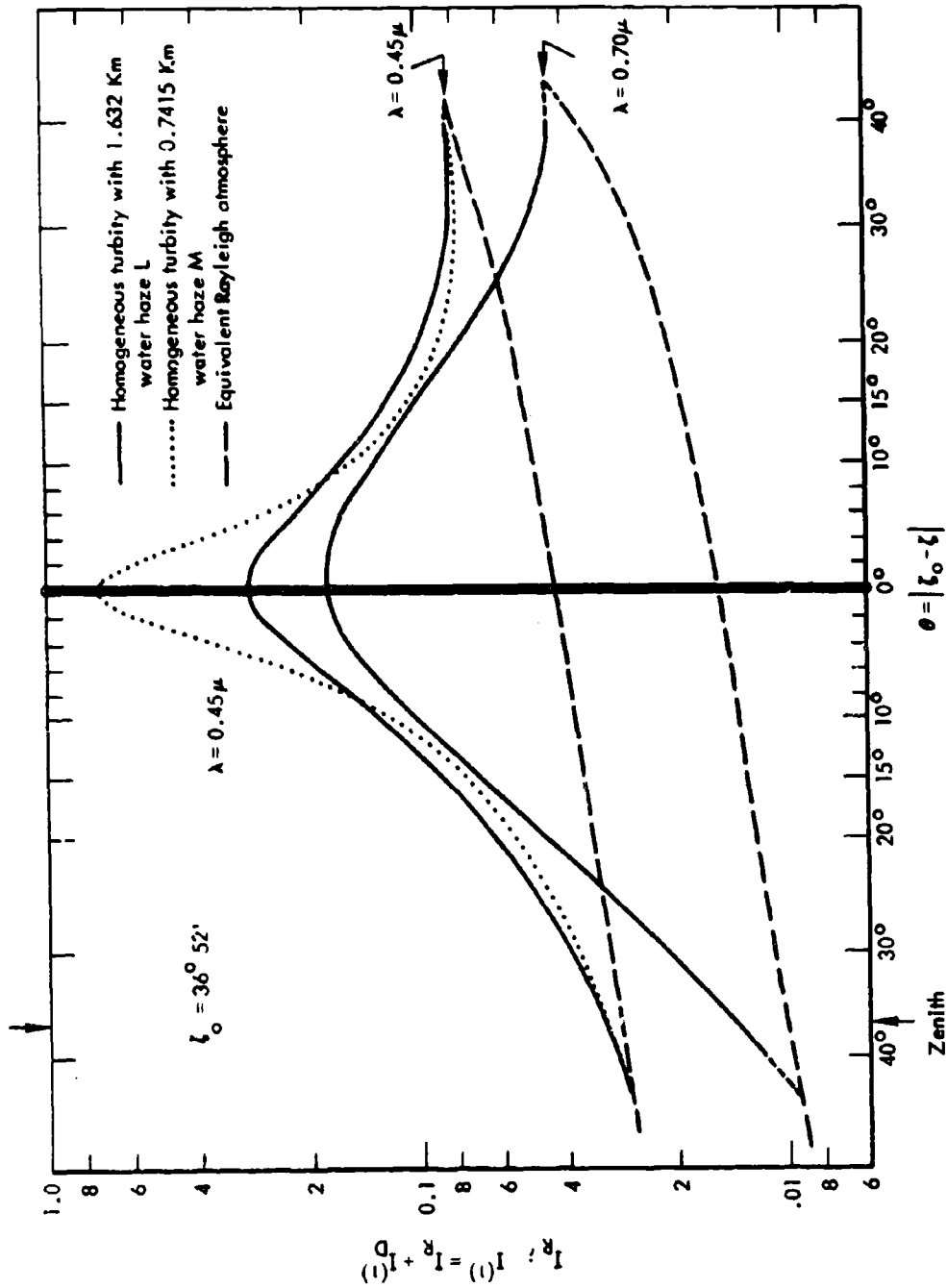
Fig. 2 -- Normalized aureole brightness (full curves) along the solar vertical, with a high sun, whose position and size are indicated by the three vertical lines at $\theta = 0°$. The abcissas are plotted linearly in terms of $\sin \theta$ (not shown), and the horizon is towards the right side of the diagram.
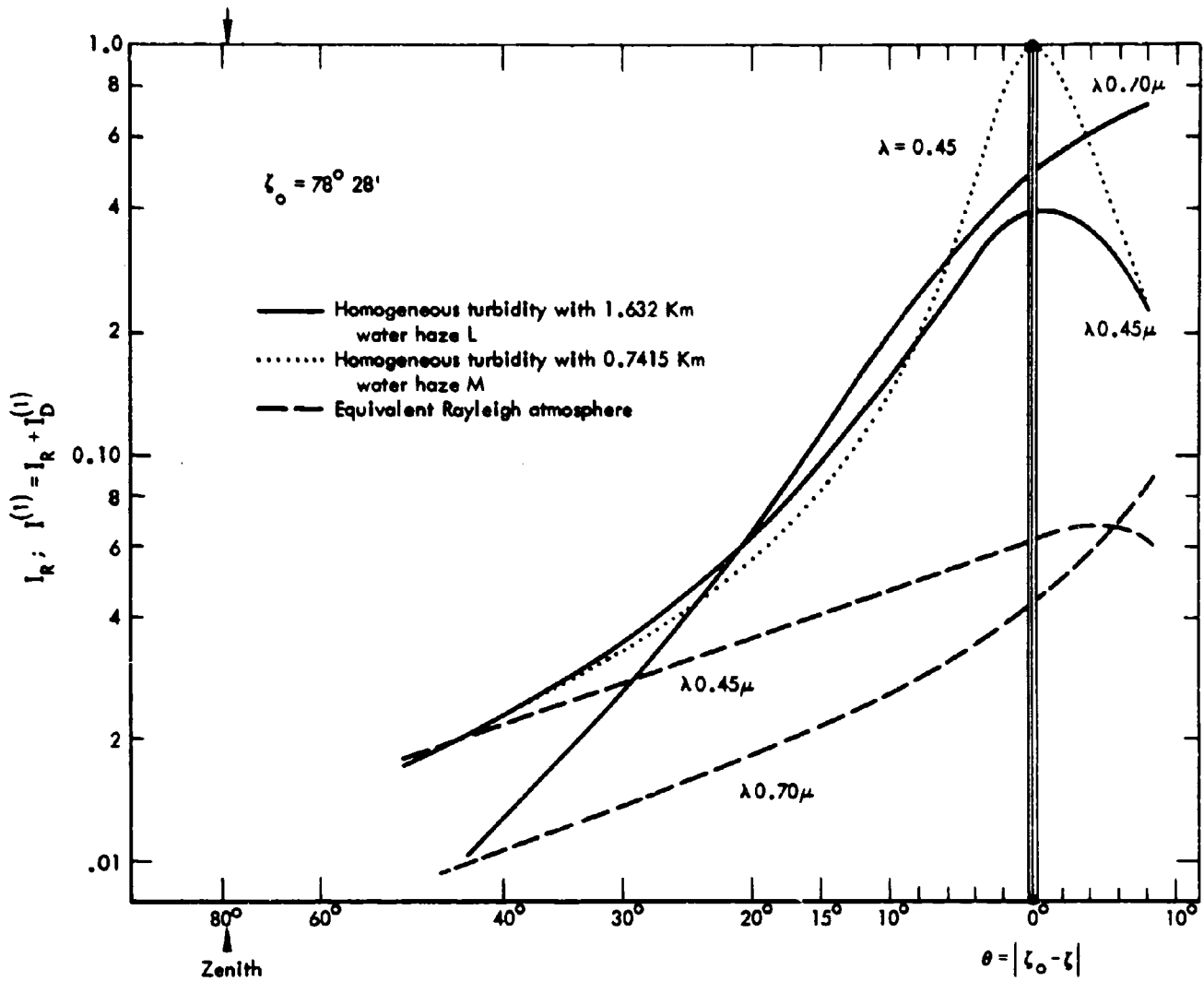
Fig 3. -- Same as Fig. 2 but for low sun.

Figure 2 represents conditions along the sun's vertical plane
with the sun at a moderate zenith distance of 36°52'. The Rayleigh
background, indicated by the dashed curves, shows the above-mentioned
smooth nature of this idealized field and its monotonic increase to-
ward the horizon at both wavelengths, characteristic of the model.
The blue Rayleigh background should be some three times as bright as
the red, that is, a factor which is only about one half of that corres-
ponding to the λ^{-4} law at these wavelengths. (Both factors should be
increased by about 4/3 when one considers the actual solar spectral
brightness.)

The full curves in Fig. 2 represent the perturbed brightness field.
Taking into account the coordinate system used in plotting these, sev-
eral points can be made about the present model of the aureoled sky in
comparison to our earlier estimate (Deirmendjian, 1959, Fig. 7) for
closely similar turbidity conditions: (a) The aureole effect should
extend to a disc of some 40° angular radius (rather than the 10° orig-
inally estimated). (b) Within a disc of radius 2° to 3° about the sun,
the aureole should show an almost constant brightness (rather than a
θ^{-1} variation, as previously suggested) which is about seven times
that of the equivalent Rayleigh atmosphere at $\lambda 0.45\mu$, and eleven times
that at $\lambda 0.70\mu$. (c) Within a ring about 10° wide in the 3° < θ < 13°
region for $\lambda 0.45\mu$, and about 20° wide in the 8° < θ < 28° region for
$\lambda 0.70\mu$, the brightness gradient could be closely approximated by a
$(\sin \theta)^{-a(\lambda)}$ variation where $a(\lambda)$ is a positive constant at each wave-
length and is determined by the size distribution of the aerosols.
In this same region the dilution of the Rayleigh-type skylight blue is
greatest, the ratio of relative intensities at $\lambda 0.45\mu$ and $\lambda 0.70\mu$ being
reduced to about 1.2 from its undiluted value of 3. At a distance of
about 40° from the sun in any direction the effects of light-to-moderate
turbidity, both on the brightness and the color of the sunlit sky,
should be negligible.

Interestingly, the region of scattering angles 40° ≤ θ ≤ 45° hap-
pens to be the same one in which it has been found that the normalized
phase function for the intensity in polydisperse scattering should be
invariant with respect to the nature of the distribution function

(Deirmendjian, 1964). Thus, under clear sky conditions, in order to
estimate the degree of atmospheric turbidity from the sky brightness
alone, measurements should be concentrated around points of the sky
corresponding to, say, $30° \leq \theta \leq 40°$, or where positive deviations
from the Rayleigh type of background just begin to appear. This cri-
terion, of course, does not apply to laboratory work with polydisperse
aerosols illuminated by a collimated beam, in which case, due to the
above-mentioned invariance, the amount of light scattered at $40°$ to
$45°$ should be directly proportional to the total number of particles
regardless of the shape of the phase function.

Figure 3 describes the aureole effect under low-sun conditions
for the same atmospheric model as for Fig. 2. The sun is now assumed
to be only about $12°$ above the horizon of a flat atmosphere; the man-
ner of plotting is the same as before except that the curves are in-
terrupted at a zenith distance of about $86°$ beyond which the effects
of sphericity become predominant. Here again there are several dif-
ferences from the earlier estimate (compare Deirmendjian 1959, e.g.
Fig. 8) and of course from the high sun situation of Fig. 2. The most
striking features revealed by Fig. 3 are (a) the gradual reddening of
the circumsolar sky as the sun approaches the horizon, with a maximum
effect near the horizon below the sun; and (b) the absence of a true
aureole at $\lambda 0.70\mu$, where the sharp increase in brightness, observed
as the sun is approached from the zenith side, persists right through
the sun's position and below, toward the horizon. Whereas it will be
agreed that feature (a) is a common phenomenon of clear, fair-weather
skies, feature (b) is difficult to assess visually. It would be in-
teresting to see whether it may be verified by photometric observations
(we are not aware of any such published observations). At any rate,
this feature may be partly spurious and due to the neglect of spher-
icity in modelling the terrestrial atmosphere, since the Rayleigh sky
(dashed curves) also shows a slight horizon reddening.

The effect on the aureole of changes in the size distribution of
the aerosols — other things remaining equal — may be evaluated by
reworking the above example, for, say, a haze-M distribution (ESSP,
pp. 78-79, and Tables T.1, T.2). To obtain the same degree of turbidity

as before, for example at $\lambda 0.45\mu$, we note that one needs less than one-half the total number of particles considered before, or $7.415 \cdot 10^6$ instead of $1.632 \cdot 10^7$) per cm^2 column. (At $\lambda 0.70\mu$ the number will be even smaller, as may be seen from a comparison of the corresponding values of β_{sc} listed in the tables.) These differences are due to the greater proportion of large aerosols incorporated in the M-type distribution than in the L-type. This also accounts for the steeper and narrower forward scattering "neck" in the $0 < \theta < 10°$ region displayed by the normalized intensity function for haze M when compared to that for haze L.

The nature of the $\lambda 0.45\mu$ aureole resulting from the substitution of an equivalent amount of haze M for haze L, other variables being exactly the same as before, is indicated by the dotted curves in Figs. 2 and 3. (The $\lambda 0.70\mu$ case is not shown since, as mentioned above, the relative contribution of the aerosols to the total optical thickness at this wavelength will not be the same as in the previous model, and hence the Rayleigh background at $\lambda 0.70\mu$ will not be that shown in Figs. 2 and 3.) The principal effects of the above substitution may be described as follows: (a) the overall extent of the aureole -- at least as far as first-order effects are concerned -- remains the same, i.e., within a ring of radius 40° to 50° around the sun; (b) the previously mentioned region, displaying a $(\sin \theta)^{-a(\lambda)}$ variation in brightness, is shifted closer to the sun, it is reduced in width from 20° to about 8°, and the slope, given by $a(\lambda)$, is considerably increased; and (c) the steep brightness gradient continues almost to the sun's limb, so that the disc of constant brightness around the sun, noted in the previous example, is eliminated. Similar effects should appear in the case of the $\lambda 0.70\mu$ aureole. In addition, as indicated by the dotted curve on Fig. 3, a distinct aureole region should persist as the sun approaches the horizon, in contrast to the previous case where the aureole is washed out at the longer wavelength.

At any rate, it is quite clear from these examples that the brightness gradient in the inner aureole region of $0 \lesssim \theta \lesssim 10°$ is the best indicator of the size distribution of the responsible particles, particularly the relative content of larger aerosols. And the overall

extent of the aureole should indicate the degree of turbidity. These conclusions will be less and less valid as the turbidity increases and orders of scattering higher than the first become relatively more important.

2.24 <u>Aureole effects for absorbing aerosols</u>. To obtain an example of the aureole as a perturbation produced by absorbing aerosols, we consider the first-order term in the appropriate equation, (19):

$$\frac{dI_D}{\sec \zeta \, d\tau} = I_D - \frac{\omega(\tau)f(\tau)}{4\pi} e^{-\tau \sec \zeta_o} P_D(\theta) \cdot F_o \qquad (30)$$

The solution is given by the expression (23), except that the transmission function in this case is given by the integral

$$T_D(\tau_1,\zeta_o,\zeta,\omega) = \sec \zeta \, e^{-\tau_1 \sec \zeta} \int_0^{\tau_1} \omega(\tau)f(\tau) \, e^{-(\sec\zeta_o-\sec\zeta)} \, d\tau \qquad (31)$$

instead of by Eq. (24), and the optical thickness is understood to include contributions by the absorption within the particles. In the real, inhomogeneous atmosphere, the integrand in Eq. (31) may be a rather complicated function of τ, since $\omega(\tau)$ and $f(\tau)$ may not vary in the same manner.

Proceeding as before, we may again assume homogeneous turbidity defined by the condition (25), which, with the help of (20), becomes

$$\omega(\tau)f(\tau) = \frac{\tau_{1scM}}{\tau_{1R} + \tau_{1M}} = \alpha_M(\tau_1) = const. \qquad (32)$$

With this condition the integration in Eq. (31) can be carried out, and we have

$$T_D(\tau_1,\zeta_o,\zeta,\alpha_M) = \frac{\sec \zeta}{|\sec \zeta - \sec \zeta_o|} \alpha_M(\tau_1) \left| e^{-\tau_1 \sec \zeta_o} - e^{-\tau_1 \sec \zeta} \right|$$

$$(33)$$

as the transmission for the perturbation in the case of absorbing
aerosols. This is seen to be analogous to Eq. (26), except that the
turbidity coefficient is here replaced by the partial albedo of single
scattering of the aerosols. Since according to Eq. (20) $\alpha_M < f(\tau)$,
it is clear that given two types of turbidity of the same degree, i.e.
having the same partial optical thickness τ_M, the one containing ab-
sorbing aerosols will produce a smaller brightness perturbation than
the one with nonabsorbing aerosols. (By the same token the higher-
order terms in the perturbation equation (19) will have an even smaller
effect under these conditions.)

For simplicity and easy comparison, let us construct a homoge-
neously turbid model of the atmosphere containing aerosols with the
same distribution as before, i.e., haze L as given by (28). As an ex-
treme example of absorbing particles, let us further consider what we
have called "iron particles," using their tabulated scattering proper-
ties at $\lambda 0.441\mu$ and $\lambda 0.668\mu$ (EESP tables T.115 and T.116).

For the Rayleigh background in this model, we would have to con-
sider the diffuse transmission for multiple scattering with $\varpi < 1$.
However, in this case the absence of detailed published data, tabulated
as a function of optical thickness and ϖ, prevents us from interpolat-
ing as before. Since in the model we wish to consider, the overall
albedo of single scattering cannot be much smaller than unity, we shall
assume the Rayleigh brightness corresponding to the conservative case
with an optical thickness given by the actual *scattering optical thick-
ness*, $\tau_{1sc} = \varpi\tau_1$, to be a good approximation to the Rayleigh background.
Furthermore, to avoid further interpolation, we choose a turbidity for
which the resulting scattering optical thicknesses are close to those
used in the previous section. To do this, it turns out that we need
an aerosol atmosphere equivalent to a 1.966-km layer of the above-
mentioned composition and number density. From the cited tables, and
by interpolation, the pertinent parameters are as follows:

Parameter	$\lambda 0.441\mu$	$\lambda 0.668\mu$
τ_{1R}	0.240	0.0435
τ_{1M} (iron "haze L")	0.0951	0.1020
τ_1	0.3351	0.1455
$f(\tau_1)$	0.1817	0.5735
ϖ_R	0.716	0.299
ϖ_M	0.159	0.402
ϖ	0.875	0.701
$\varpi \tau_1 = \tau_{1sc}$	0.2932	0.1020

It is seen that the values in the last row are quite close to those of the total optical thickness used in the example of the previous section. We shall therefore use the same Rayleigh backgrounds indicated in Figs. 2 and 3, without further modification, and evaluate the expected perturbation from an absorbing aerosol as before.

Note, by the way, that the partial albedo of single scattering ϖ_M for aerosols, as here defined, is not the same as that of the particles themselves (e.g. 0.5604 and 0.5736, respectively, at $\lambda 0.441\mu$ and $\lambda 0.668\mu$, in this case according to ESSP, T.115 and T.116), but depends on the turbidity coefficient as well as on the absorbing properties of the particles. In the above example it is seen that the value of ϖ_M at $\lambda 0.441\mu$ is less than one-half that at $\lambda 0.668\mu$ (despite the fact the particle albedos are practically equal at these wavelengths) and hence, by virtue of Eq. (33), the corresponding perturbations will be in the same ratio.

The perturbed field corresponding to this example is depicted in Figs. 4 and 5, which are plotted on the same basis as Figs. 2 and 3. At first glance the general features of the aureole produced by absorbing and nonabsorbing aerosols seem to be quite similar. On closer examination, however, significant differences may be seen. Most notable are the decreased extent and reduced brightness of aureoled sky,
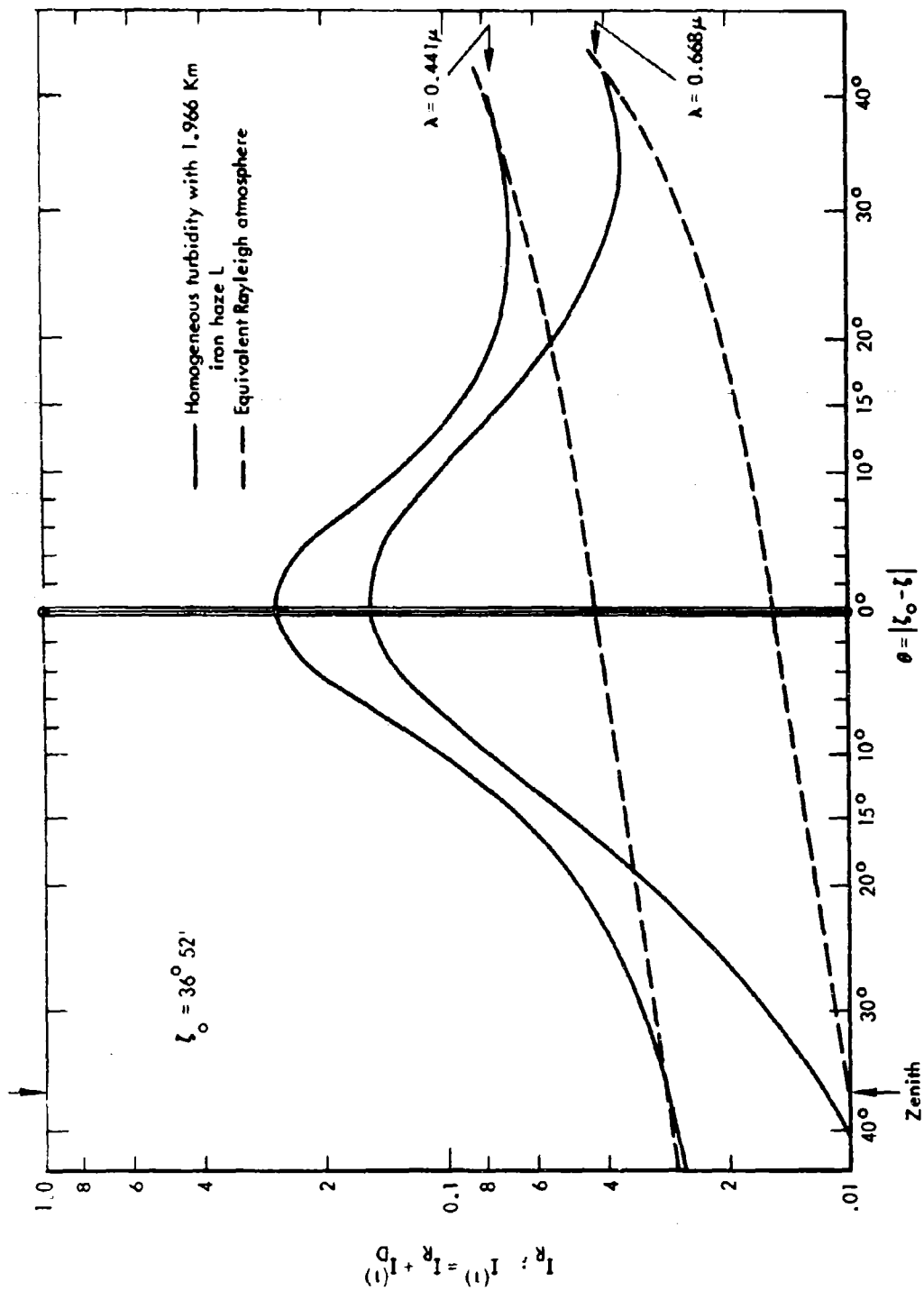
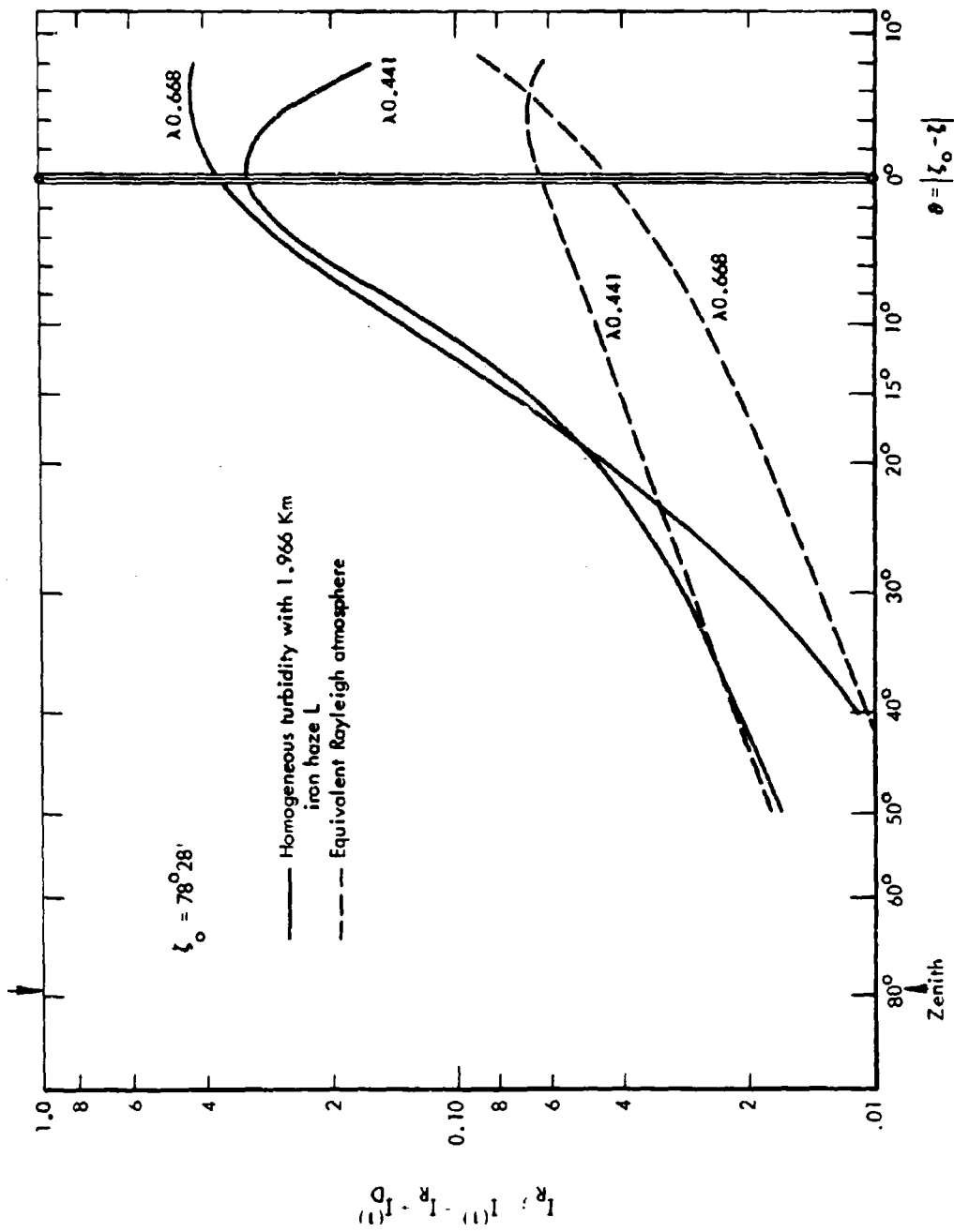Fig. 4 -- Same as Fig. 2 but for strongly absorbing aerosols.

Fig. 5 -- Same as Fig. 3 but for strongly absorbing aerosols.

by twenty percent and more in the typical regions of 10° above and below the sun (compare homologous values in the corresponding tables of the Appendix). This reduction is greatest near the horizon at $\lambda 0.668\mu$, when the sun is low.

It is noteworthy that even though the scattering optical thickness has been taken equal to that of the previous example (Section 2.23), the assumption of absorbing aerosols results in an overall reduction of sky brightness, mostly in the broad aureole region, without a compensatory increase in other directions. The amount of this reduction, which corresponds to the energy absorbed within the particles and presumably used in raising their temperature, exceeds that expected from the difference $1 - \varpi$, where ϖ is the albedo of single scattering of the mixed atmosphere (compare the values 0.125 and 0.299 at the two reference wavelengths with the reductions indicated by the tables in the Appendix). This excess must be due to the fact that the absorption operates not only on the direct but also on the singly scattered sunlight. The overall absorption, of course, depends not only on $1 - \varpi$ and the turbidity, $f(\tau)$, but also on the inclination of the sun's "rays" or ζ_o.

These simple conclusions, based on first-order perturbation theory and a homogeneous model of the turbid atmosphere, are consistent with observation, and clarify certain effects, some of which may become more pronounced when higher orders of scattering are included. For example, one may make initial estimates of radiative heating caused by the presence of absorbing aerosols by constructing similar models for various types and amounts of turbidity.

2.25 <u>Comparison with observations</u>. The degree of validity of the above-described models of the clear-sky aureole cannot be judged until they are compared with actual observations. A number of authors have published the results of recent observations. We wish to mention those described by Eiden (1968), carried out both near industrial centers in Germany and at a high mountain station in Hawaii, and by Sekihara and Murai (1961) in Japan. The more detailed results presented by K. Murai (1967, 1968) deserve particular mention. In general these observations

confirm the validity of the present models and the method of analysis.
A more detailed comparison is planned for future study.

Another recent piece of work by Rydgren (1968) is confined to the
innermost aureole, in a region not exceeding 1°06' from the sun's limb,
which of course represents only a small portion of the entire aureole
perturbation.

2.3 Diffuse Reflection on a Turbid Atmosphere

The first-order perturbation method could, of course, be used in
considering large-angle scattering problems, and in particular the
diffuse reflection of sunlight in the case of a moderately turbid at-
mosphere. Provided ground reflection is neglected, the corresponding
solution, in the case of homogeneous turbidity, would be very similar
to Eq. (27), with the proper transmission function T_D obtained by an-
alogy with Eq. (3). This is in fact the method used by Livshits
(1969) -- who seems to be ignorant of our initial introduction of the
method (Deirmendjian 1957, 1959) -- in an attempt to estimate the de-
gree of polarization of the diffusely reflected sunlight.

In our opinion the method is hardly adequate for the treatment of
this problem, particularly in polarization and neutral-point studies,
where multiple scattering must be considered. Most important, unless
the ground-reflection effects are introduced rather accurately, in-
cluding the polarization and angular variation introduced by the par-
ticular reflection mechanism, it is doubtful that even the intensity
of diffuse reflection can be explained satisfactorily by this type of
perturbation treatment. However, with some modification to account
for sphericity, the method may be adequate in an initial interpretation
of certain low-orbit satellite observations with the sun close to the
horizon.

3. SUMMARY AND FURTHER REMARKS

In this first part of a review of primary scattering techniques in cloud microphysics research, we have outlined the use of exact Mie theory phase functions for idealized polydispersions representing aerosols in a perturbation method to account for the circumsolar aureole. Certain shortcomings of an earlier application of the method have been pointed out and corrected. In addition, the method has been extended to include absorbing aerosols.

Our main conclusions are: (a) the degree of turbidity can best be assessed by comparing the deviations of sky brightness within a ring of radius 40° around the sun with the brightness corresponding to an equivalent Rayleigh atmosphere, and (b) the nature of the size distribution of the aerosol is closely related to the brightness gradient within a disc of radius 10° around the sun. Both these effects may be analyzed in terms of turbidity models based on polydispersions of Mie particles.

The method, which is appealing in its simplicity and physical clarity, should be useful in providing rough estimates of the effects of various amounts and types of turbidity on the radiation budget of the earth-atmosphere system, and hence ultimately of the climatic effects, if any, of secular changes in turbidity.

We hope to discuss other applications of scattering techniques in the light of existing experimental technology in subsequent reports.

APPENDIX

For convenience of the exigent reader, under Tables 2 and 3 we list the actual values of the sky brightness computed for the models and by the method outlined in Sections 2.23 and 2.24. These values are those plotted in Figs. 2, 3, 4, and 5.

Table 2

PERTURBED SKY BRIGHTNESS VALUES $I_R + I_D^{(1)}$

ζ_o = arc cos (0.80) $\doteq$ 36°52'

$\theta = \|\zeta_o - \zeta\|$		With Water Haze L		With Iron Haze L	
	$\lambda(\mu)$:	0.45	0.70	0.441	0.668
	ϖ :	1.0	1.0	0.875	0.701
sun above — 40°		0.0293	0.0117	0.0276	0.0104
30		0.0393	0.0212	0.0330	0.0161
20		0.0625	0.0454	0.0474	0.0319
15		0.0869	0.0688	0.0660	0.0498
10		0.1322	0.1040	0.1073	0.0809
8		0.1592	0.1223	0.1355	0.0974
6		0.1935	0.1393	0.1722	0.1159
5		0.2136	0.1485	0.1925	0.1248
4		0.2336	0.1573	0.2130	0.1334
3		0.2523	0.1631	0.2311	0.1402
2		0.2701	0.1698	0.2468	0.1460
1		0.2816	0.1747	0.2584	0.1512
0		0.2871	0.1786	0.2648	0.1540
sun below — 1		0.2878	0.1790	0.2639	0.1549
2		0.2821	0.1783	0.2575	0.1530
3		0.2693	0.1756	0.2465	0.1506
4		0.2548	0.1735	0.2319	0.1469
5		0.2382	0.1679	0.2142	0.1406
6		0.2205	0.1617	0.1959	0.1339
8		0.1898	0.1491	0.1611	0.1182
10		0.1652	0.1336	0.1336	0.1033
15		0.1220	0.1008	0.0925	0.0723
20		0.0990	0.0766	0.0752	0.0533
30		0.0818	0.0503	0.0689	0.0377
40		0.0828	0.0435	0.0775	0.0384

Table 3

PERTURBED SKY BRIGHTNESS VALUES $I_R + I_D^{(1)}$

ζ_o = arc cos (0.20) $\doteq$ 78°28'

$\theta = \|\zeta_o - \zeta\|$		With Water Haze L		With Iron Haze L	
	$\lambda(\mu)$:	0.45	0.70	0.441	0.668
	ϖ :	1.0	1.0	0.875	0.701
50°		0.0168	0.0074	0.0168	0.0077
40		0.0227	0.0125	0.0213	0.0110
30		0.0342	0.0262	0.0289	0.0193
20		0.0623	0.0666	0.0467	0.0442
15		0.0929	0.1126	0.0684	0.0754
10		0.1525	0.1949	0.1164	0.1366
8		0.1896	0.2431	0.1499	0.1743
6		0.2380	0.2967	0.1943	0.2200
5		0.2672	0.3277	0.2191	0.2442
4		0.2968	0.3578	0.2447	0.2704
3		0.3258	0.3901	0.2682	0.2941
2		0.3542	0.4244	0.2890	0.3180
1		0.3749	0.4575	0.3051	0.3430
0		0.3876	0.4922	0.3149	0.3644
1		0.3930	0.5205	0.3153	0.3836
2		0.3885	0.5498	0.3081	0.3979
3		0.3723	0.5759	0.2939	0.4116
4		0.3514	0.6034	0.2739	0.4229
5		0.3245	0.6332	0.2481	0.4278
6		0.2923	0.6587	0.2194	0.4305
8		0.2249	0.7169	0.1609	0.4204

(rows 50° through 1 marked "above sun"; rows 1 through 8 marked "below sun")

REFERENCES

Coulson, K. L., Dave, J. V., and Sekera, Z. 1960. *Tables Related to Radiation Emerging from a Planetary Atmosphere with Rayleigh Scattering*. University of California Press, Berkeley.

Deirmendjian, D. 1955. The optical thickness of the molecular atmosphere. *Archiv. Meteor. Geophys. Bioklim.* B.6 (4), 452-461.

Deirmendjian, D. 1956. *Atmospheric Scattering of Light and the Sun's Aureole*. Dissertation, University of California, Los Angeles.

Deirmendjian, D. 1957. Theory of the solar aureole, I. *Ann. Géoph.* 13, 286-306.

Deirmendjian, D. 1957. Theory of the solar aureole, II. *Ann. Géoph.* 15, 218-249.

Deirmendjian, D. 1963. Scattering and polarization properties of polydisperse suspensions with partial absorption, in *I.C.E.S.*, M. Kerker, ed., pp. 171-189, Pergamon Press, Oxford.

Deirmendjian, D. 1964. Scattering and polarization properties of water clouds and hazes in the visible and infrared. *Appl. Optics* 3, 187-196.

Deirmendjian, D. 1969. *Electromagnetic Scattering on Spherical Polydispersions*. American Elsevier, New York; also *Electromagnetic Scattering on Spherical Polydispersions*. R-456-PR, The Rand Corporation, Santa Monica, California.

Deirmendjian, D., and Sekera, Z. 1953. Quantitative evaluation of multiply scattered and diffusely reflected light. *J. Opt. Soc. Amer.* 43, 1158-1165.

Eiden, R. 1968. Calculations and measurements of the spectral radiance of the solar aureole. *Tellus* 20, 380-399.

Elterman, L. 1964a. Parameters for attenuation in the atmospheric windows for fifteen wavelengths. *Appl. Optics* 3, 745-749.

Elterman, L. 1964b. *Atmospheric Attenuation Model, 1964, in the Ultraviolet, Visible, and Infrared Regions for Altitudes to 50 Km*. Env. Res. Paper No. 46, A.F.C.R.L., Bedford, Mass.

Livshits, G. Sh. 1969. An approximate method of calculating the degree of polarization of upward atmospheric radiation in the solar vertical. *Atmos. Ocean. Phys.* 5, 453-456 (transl. from the Russian original).

Murai, Keizo. 1967. Spectral measurements of direct solar radiation and of the sun's aureole (I). *Papers in Meteor. and Geophys.* 18 (3), 239-291.

Murai, Keizo. 1968. Spectral measurements of direct solar radiation and of the sun's aureole (II). *Papers in Meteor. and Geophys.* 19 (3), 447-480.

Rozenberg, G. V. 1968. Optical investigations of atmospheric aerosol. *Soviet Physics Uspekhi* 11, 353-380 (transl. from the Russian).

Rydgren, Bo. 1968. A photometric study of the solar aureole under various weather conditions. *Tellus* 20, 55-64.

Sekera, Z. 1956. Recent developments in the study of the polarization of skylight. *Adv. Geophys.* 3, 43-104.

Sekera, Z., and Kahle, A. B. 1966. *Scattering Functions for Rayleigh Atmospheres of Arbitrary Thickness.* R-452-PR, The Rand Corporation, Santa Monica, California.

Sekihara, K., and Murai, K. 1961. On the measurement of atmospheric extinction of solar radiation and the sun's aureole. *Papers in Meteor. and Geophys.* 19 (1), 57-74.

DOCUMENT CONTROL DATA

1. ORIGINATING ACTIVITY	2a. REPORT SECURITY CLASSIFICATION
The Rand Corporation	UNCLASSIFIED
	2b. GROUP

3. REPORT TITLE

USE OF SCATTERING TECHNIQUES IN CLOUD MICROPHYSICS RESEARCH I. THE AUREOLE METHOD

4. AUTHOR(S) (Last name, first name, initial)

Deirmendjian, D.

5. REPORT DATE	6a. TOTAL NO. OF PAGES	6b. NO. OF REFS.
October 1970	48	20

7. CONTRACT OR GRANT NO.	8. ORIGINATOR'S REPORT NO.
F44620-67-C-0045	R-590-PR

9a. AVAILABILITY/LIMITATION NOTICES	9b. SPONSORING AGENCY
DDC-1	United States Air Force Project RAND

10. ABSTRACT

A simple, physically clear method for assessing the amount of atmospheric turbidity on a cloudless day by observing the circumsolar aureole--the ring of brightness around the sun--and comparing its brightness with that of the equivalent Rayleigh scattering (particle-free) atmosphere. The aureole is known to be caused by aerosols. This report applies exact Mie theory phase functions for idealized polydispersions of spherical particles to account for the aureole. It shows that the brightness gradient within a disc of 10-deg radius around the sun indicates the size distribution of the aerosol particles, and the overall extent of the aureole within 40 deg around the sun indicates the degree of turbidity. These conclusions will apply less and less as turbidity increases and higher orders of scattering become more important. With some modifications to account for the earth's sphericity, the method may be adequate for initial interpretation of certain low-orbit satellite observations with the sun close to the horizon.

11. KEY WORDS

Atmosphere
Air Pollution
Meteorology
Environmental Problems